Electronic Supplementary Material (ESI) for Journal of Materials Chemistry C.

"Temperature- and pressure-dependent studies of highly flexible and compressible perovskite-like cadmium dicyanamide framework templated by protonated tetrapropylamine"

by Mirosław Mączka et al.

Table S1. The obtained parameters for the DSC measurements of TPrACd.[a]

Temperature sweep rate ($Kmin^{-1}$)	T_c (K)	ΔH ($KJmol^{-1}$)	ΔS ($Jmol^{-1}K^{-1}$)	N, by $\Delta S=RlnN$
2	387^u, 385^d 386^{av}	3.10^u, 3.09^d 3.095^{av}	8.0^u, 8.0^d 8.0^{av}	2.6
5	388^u, 384^d 386^{av}	3.15^u, 3.20^d 3.175^{av}	8.1^u, 8.3^d 8.2^{av}	2.7
10	390^u, 382^d, 386^{av}	3.30^u, 3.18^d 3.24^{av}	8.5^u, 8.3^d 8.4^{av}	2.7
2	363^u, 361^d 362^{av}	0.18^u, 0.16^d 0.17^{av}	0.50^u, 0.44^d 0.47^{av}	1.06
5	363^u, 360^d 361.5^v	0.17^u, 0.16^d 0.165^{av}	0.47^u, 0.44^d 0.455^{av}	1.06
10	365^u, 359^d, 362^{av}	0.17^u, 0.16^d 0.165^{av}	0.47^u, 0.45^d 0.46^{av}	1.06
2	242^u, 240^d 241^{av}	0.63^u, 0.62^d 0.625^{av}	2.6^u, 2.6^d 2.6^{av}	1.37
5	243^u, 240^d 241.5^{av}	0.68^u, 0.63^d 0.655^{av}	2.8^u, 2.6^d 2.7^{av}	1.38
10	244^u, 238^d 241^{av}	0.66^u, 0.69^d 0.675^{av}	2.7^u, 2.9^d 2.8^{av}	1.40
2	229^u, 228^d 228.5^{av}	1.52^u, 1.40^d 1.46^{av}	6.6^u, 6.1^d 6.35^{av}	2.1
5	230^u, 227^d 228.5^{av}	1.47^u, 1.53^d 1.50^{av}	6.4^u, 6.7^d 6.55^{av}	2.2
10	230^u, 225^d 227.5^{av}	1.52^u, 1.44^d 1.48^{av}	6.6^u, 6.4^d 6.5^{av}	2.2

[a]Sueprscripts u, d and av denote heating, cooling and average, respectively

Table S2. Room-temperature Raman wavenumbers (in cm^{-1}) of [TPrA][Cd(dca)$_3$] single crystal measured in different scattering geometries corresponding to A_1, B_1, B_2 and E Raman-active modes of the P-42$_1$c phase.[a] Modes below 100 cm^{-1} were observed with use of the eclipse filter. Modes corresponding to the dca ligand are denoted by red colour.

y(xx)y - A_1+B_1	y(zz)y - A_1	y(xz)y - E(LO)	z(xy)z - B_2(LO)	Assignment
2996w	2998w	3000w	2998w	$\nu_{as}(CH_3)$
2974m	2974m		2974w	$\nu_{as}(CH_2)$
		2954w	2958w	$\nu_{as}(CH_2)$
2941m	2941m			$\nu_{as}(CH_2)$
2934m	2932m		2936w	$\nu_{as}(CH_2)$
2910w	2910w			$\nu_s(CH_2)$
2880m	2880m	2880w	2880w	$\nu_s(CH_3)$
			2284w	$\nu_s(C\equiv N)$
2242s	2246s	2246m	2243m	$\nu_s(C\equiv N)$
2237s		2238sh	2238m	$\nu_s(C\equiv N)$
		2195w		$\nu_{as}(C\equiv N)$
2169vw				$\nu_{as}(C\equiv N)$
2156vw	2160vw	2159w	2154m	$\nu_{as}(C\equiv N)$
1461sh	1465vw			$\delta_s(CH_3)$
1453w	1454w	1453w	1453w	$\delta_s(CH_3)$
1383vw				$\omega(CH_2)$
	1352vw	1351vw		$\nu_{as}(N-C)$
1330vw	1331w		1331w	$\delta_s(CH_3)$
1319w	1314w		1319w	$\omega(CH_2)$
			1312vw	$\omega(CH_2)$

1173vw	1187vw	1173w	1172vw	$\tau(CH_2)$
1155vw			1158vw	δ(skeletal)
1141w	1139w	1139w	1138vw	δ(skeletal)
1104w	1104w	1106w	1104w	δ(skeletal)
1079vw	1079vw			overtone
1040w		1040w	1040w	δ(C-C-C)
	1034w	1032w	1032sh	δ(C-C-C)
940w	940w			δ(C-N-C)
927m	927m	928w	926w	ν_s(N-C)
			903vw	overtone
877vw		874w	871vw	ν(C-C)
848vw		847w	848w	δ(C-N-C)
784vw	783w			ν(C-N-C)
774w	777w			$\rho(CH_2)$
755w	755w	757w		$\nu(NC_4) + \rho(CH_2)$
666m	656m	658w	664w	δ_s(N-C-N)
	609vw			overtone
	541vw	540w	540w	γ_s(N-C-N)
514w		517w	513w	γ_{as}(N-C-N)
379w				$\delta(NC_4)$
363w	368w			$\delta(NC_4)$
345w			346vw	δ(skeletal)
335w		339vw	335vw	δ(skeletal)
310m	310m	309vw	310w	δ(skeletal)
	243s	243vw		T'(dca) + T'(Cd)

221s			217w	T'(dca) + T'(Cd)
198m	198s			T'(dca) + L(dca) + T'(Cd)
		164s	161s	T'(dca) + L(dca) + T'(Cd)
	134s	140sh	141sh	T'(dca) + L(dca) + T'(Cd)
115s	105w			T'(TPrA$^+$) + L(TPrA$^+$) + T'(Cd)
y(xx)y + y(zx)y A_1+B_1+ E(LO)	y(zz)y + y(xz)y A_1+E(LO)			
85w				T'(Cd)
19sh	19s			L(CdN_6)
12s				L(CdN_6)

[a]Key: s, strong; m, medium; w, weak; vw, very weak; sh, shoulder; b, broad; ν, δ, γ, ω, τ, ρ, T' and L denotes stretching, in-plane bending, out-of-plane bending, wagging, twisting, rocking, translational and librational, respectively.

Table S3. IR wavenumebrs (in cm^{-1}) of [TPrA][Cd(dca)$_3$] at 400, 300 and 80 K.[a]

400 K	300 K	80 K	Assignment
3071w,b	3068w,b	3065w,b	$\nu_{as}(CH_3)$
	3040vw	3042vw	$\nu_{as}(CH_3)$
2996m	2995m	3000sh, 2991w	$\nu_{as}(CH_3)$
2976m	2978m, 2974m	2984w, 2977m, 2972m 2963sh	$\nu_{as}(CH_2)$
2939m	2941m	2941m	$\nu_{as}(CH_2)$
2907vw	2905vw	2905w	$\nu_{s}(CH_2)$
2886sh, 2881m	2885m, 2882m	2887m, 2878m	$\nu_{s}(CH_2)$
2286m	2292m, 2286sh	2295m, 2291m	$\nu_{s}(C\equiv N)$
2264vw	2265vw	2267vw	$\nu_{s}(C\equiv N)$
		2255vw	$\nu_{s}(C\equiv N)$
2237m	2237m	2244sh, 2235m,	$\nu_{s}(C\equiv N)$
	2211w	2222vw, 2215w,	$\nu_{s}(C\equiv N)$
2173s	2174s, 2166sh	2194m, 2187m, 2176m 2170s, 2160w, 2153w	$\nu_{as}(C\equiv N)$
2137sh	2140w	2139w	$\nu_{as}(C\equiv N)$
1481sh	1481w	1473w	$\delta_{as}(CH_3)$
1471w	1472w	1468w	$\delta_{as}(CH_3)$
1459w	1462w	1452w, 1450sh	$\delta_{s}(CH_3)$
1384w	1384w	1385w	$\omega(CH_2)$
1350m	1354m	1363m, 1355m, 1351sh	$\nu_{as}(N\text{-}C)$
1326w	1326w	1326w, 1322sh	$\omega(CH_2)$
1039w	1040w	1041w	$\delta(C\text{-}C\text{-}C)$
977sh	986w	992w, 986vw, 982vw	$\delta(C\text{-}N\text{-}C) + \delta(C\text{-}C\text{-}C)$

973w	969w	972sh, 967w	δ(C-N-C) + δ(C-C-C)
922w	922w, 915w	922sh, 916w	ν_s(N-C)
871vw	872vw	973vw	ν(C-C)
844vw	850vw	850vw	δ(C-N-C)
759w	754w	758w, 747vw	$\nu(NC_4)$ + $\rho(CH_2)$
664w	660w	659w	δ_s(N-C-N)

[a]Key: s, strong; m, medium; w, weak; vw, very weak; sh, shoulder; b, broad; ν, δ, γ, ω, τ, ρ, T' and L denotes stretching, in-plane bending, out-of-plane bending, wagging, twisting, rocking, translational and librational, respectively.

Table S4. Raman wavenumbers (in cm^{-1}) of [TPrA][$Cd(dca)_3$] single crystal measured at 400, 300 and 80 K in y(zz+zx)y and y(xx+xz)y polarization configurations (notation for the room-temperature P-42_1c phase).[a]

y(zz+zx)y			y(xx+xz)y			
400 K	300 K	80 K	400 K	300 K	80 K	Assignment
2997w	2998w	3015w	2998w	2996w	3017w	$\nu_{as}(CH_3)$
		2997w			2987m	
2971m	2974m	2982sh	2971m	2974m	2973m	$\nu_{as}(CH_2)$
		2976m				
	2952vw	2967w		2953vw		$\nu_{as}(CH_2)$
		2957w				
2940m	2941m	2946m	2939m	2941m	2955m	$\nu_{as}(CH_2)$
2931m	2932m	2934m		2934m	2934m	$\nu_{as}(CH_2)$
2908sh	2910w	2914w	2908w	2910w	2900vw	$\nu_{s}(CH_2)$
		2900w				
2880m	2880m	2879m	2880m	2880m	2878m	$\nu_{s}(CH_3)$
		2296w			2292w	$\nu_{s}(C\equiv N)$
2235s	2246s	2948s	2243s	2242s	2246s	$\nu_{s}(C\equiv N)$
					2242s	
	2239sh	2944sh	2236sh	2237s	2234m	$\nu_{s}(C\equiv N)$
		2197w			2198w	$\nu_{as}(C\equiv N)$
		2177w		2169vw	2176w	$\nu_{as}(C\equiv N)$
		2169w			2169w	
2166vw	2160vw	2160w	2158w	2156vw	2160w	$\nu_{as}(C\equiv N)$
					2153w	
1464sh	1465sh	1466w	1467sh	1462sh	1466w	$\delta_{s}(CH_3)$
1454w	1454w	1452w	1452w	1453w	1453w	$\delta_{s}(CH_3)$
			1390vw	1387vw	1386vw	$\omega(CH_2)$
1350vw	1352vw	1353w		1350vw	1354vw	$\nu_{as}(N\text{-}C)$
1331w	1331w	1335w		1331vw	1334w	$\delta_{s}(CH_3)$
1315w	1314w	1317w	1322vw	1318w	1308w	$\omega(CH_2)$
		1308w				

		1291vw			1272vw	ω(CH_2)
	1187vw					τ(CH_2)
1167vw	1170vw	1174w	1170w	1173vw	1176w	τ(CH_2)
		1153vw		1155vw	1154vw	δ(skeletal)
1137w	1139w	1142vw	1137w	1139w		δ(skeletal)
1103w	1104w	1106w	1101w	1104w	1108w	δ(skeletal)
					1103sh	
1074w	1078vw	1077w				overtone
1033w	1034w	1043w	1035m	1040w	1044w	δ(C-C-C)
		1034w			1034w	
		991vw			990vw	δ(C-N-C) + δ(C-C-C)
	940sh	943w		940sh	943vw	δ(C-N-C)
929m	927m	928m	928m	927m	928m	ν_s(N-C)
		921w			923sh	
868vw	873vw	873w	871w	873w	875w	ν(C-C)
846w	847w	852w	845w	848w		δ(C-N-C)
	783w	786m			785w	ν(C-N-C)
775w	777w	766w	773w	775w		ρ(CH_2)
757w	755w	744w	752w	756w	758vw	ν(NC_4) + ρ(CH_2)
					745vw	
658m	656m	662sh	667m	665m	666m	δ_s(N-C-N)
		651m			658sh	
		557w			549vw	γ_s(N-C-N)
		549w				
536vw	539vw	537w	534w	539w	537vw	δ_{as}(N-C-N)
	514vw	513w	514w	515w	523vw	γ_{as}(N-C-N)
					513vw	
				376w		δ(NC_4)

365w	368w			361w	363w	$\delta(NC_4)$
	343vw			345w	350w	δ(skeletal)
			337w	333w	339w	δ(skeletal)
309m	310m	313m	309m	310m	316m	δ(skeletal)
					312m	
240sh	243s	261m			260w	T'(dca) + T'(Cd)
		231m			228m	
	213sh	212w	219s	219s	212m	T'(dca) + T'(Cd)
		204w			206m	
197s	196s	176s		194m	179m	T'(dca) + L(dca) + T'(Cd)
	162sh	163m		165s	158w	T'(dca) + L(dca) + T'(Cd)
142s	134s	140m	144s	130m	125m	T'(dca) + L(dca) + T'(Cd)
117sh		130m	123sh			
	103w	116vw		114s	110w	$T'(TPrA^+)$ + $L(TPrA^+)$ + T'(Cd)
		95m			67w	
		67w				

[a]Key: s, strong; m, medium; w, weak; vw, very weak; sh, shoulder; b, broad; ν, δ, γ, ω, τ, ρ, T' and L denotes stretching, in-plane bending, out-of-plane bending, wagging, twisting, rocking, translational and librational, respectively.

Table S5. Lattice parameters of $[TPrA][Cd(dca)_3]$ as a function of pressure.

phase	P (GPa)	a (Å)	b (Å)	c (Å)	α (°)	β (°)	γ (°)	V (Å)
I	0	16.317(1)	16.317(1)	17.590(1)	90	90	90	4683.2(1)

	0.2	16.294(1)	16.294(1)	17.589(1)	90	90	90	4670.0(1)
II	0.8	16.077(1)	15.486(1)	17.464(1)	90	90.192(6)	90	4348.2(1)
	1.3	15.884(1)	15.200(1)	17.330(1)	90	90.316(3)	90	4184.1(1)
	1.8	15.800(1)	15.013(1)	17.250(1)	90	90.462(3)	90	4091.8(1)
	2.3	15.692(1)	14.903(1)	17.154(1)	90	90.614(8)	90	4011.3(1)
	2.8	15.623(1)	14.763(1)	17.057(1)	90	90.689(8)	90	3934.0(1)
	3.3	15.537(1)	14.627(1)	16.949(1)	90	90.732(8)	90	3851.6(1)
	3.8	15.470(1)	14.534(1)	16.862(1)	90	90.777(2)	90	3791.0(1)
	4.3	15.421(1)	14.451(1)	16.795(1)	90	90.838(6)	90	3742.4(1)
	5.0	15.368(1)	14.362(1	16.725(1)	90	90.868(9)	90	3691.3(1)
	6.0	15.293(1)	14.284(1)	16.633(1)	90	90.880(3)	90	3633.8(1)

Table S6. Wavenumber intercepts at zero pressure (ω_0) and pressure coefficients ($\alpha=d\omega/dP$), obtained from fitting of the experimental data by linear functions, for the three phases of [TPrA][Cd(dca)$_3$].

ambient pressure phase		high-pressure phase		high-pressure phase		assignment
ω_0 (cm^{-1})	α ($cm^{-1}GPa^{-1}$)	ω_0 (cm^{-1})	α ($cm^{-1}GPa^{-1}$)	ω_0 (cm^{-1})	α ($cm^{-1}GPa^{-1}$)	
2246.2	6.7	2243.5	7.2	2244.3	7.3	ν_s(C≡N)
2238.4	4.1	2238.2	5.4	2241.8	4.4	ν_s(C≡N)
		2175.5	4.3			ν_{as}(C≡N)
2158.1	3.4	2157.7	6.7	2169.4	3.4	ν_{as}(C≡N)
1173.0	6.5	1174.6	2.4	1171.5	2.5	$\tau(CH_2)$
1155.2	6.5	1155.8	2.9			δ(skeletal)
1142.1	0.7	1139.3	2.6	1138.4	3.6	δ(skeletal)
1106.9	2.8	1107.1	2.3	1102.3	3.3	δ(skeletal)
1078.0	8.8					overtone
1040.2	7.1	1041.1	5.0	1040.3	5.5	δ(C-C-C)
928.4	5.2	928.5	4.4	928.2	5.1	ν_s(N-C)
				919.8	3.7	ν_s(N-C)
874.4	6.0	875.0	3.0	877.3	2.6	ν(C-C)
849.4	2.7	849.8	6.8	848.9	6.0	δ(C-N-C)
775.7	6.1	782.0	3.4	776.1	5.3	$\rho(CH_2)$
757.2	2.0	760.7	0.9	757.5	1.7	$\nu(NC_4) + \rho(CH_2)$
664.0	4.2	665.0	2.9	669.2	0.5	δ_s(N-C-N)
		653.5	2.5	660.1	-0.9	δ_s(N-C-N)
540.2	7.9	536.5	2.6	533.8	3.2	δ_{as}(N-C-N)
517.1	2.2	510.7	1.2	510.1	1.4	γ_{as}(N-C-N)
367.1	28.4					$\delta(NC_4)$
341.3	6.9	345.7	4.5	335.5	7.9	δ(skeletal)
312.9	2.9	315.0	5.3	308.3	7.0	δ(skeletal)
246.8	8.0	230.2	8.7	224.2	9.5	T'(dca) + T'(Cd)
222.1	2.1	213.9	4.1			T'(dca) + T'(Cd)
199.7	14.5					T'(dca) + L(dca) + T'(Cd)
166.7	0.1	177.7	9.8	189.8	5.3	T'(dca) + L(dca) + T'(Cd)
142.5	2.6	140.6	5.8	139.9	5.0	T'(dca) + L(dca) + T'(Cd)
		120.9	4.8			T'(dca) + L(dca) + T'(Cd)

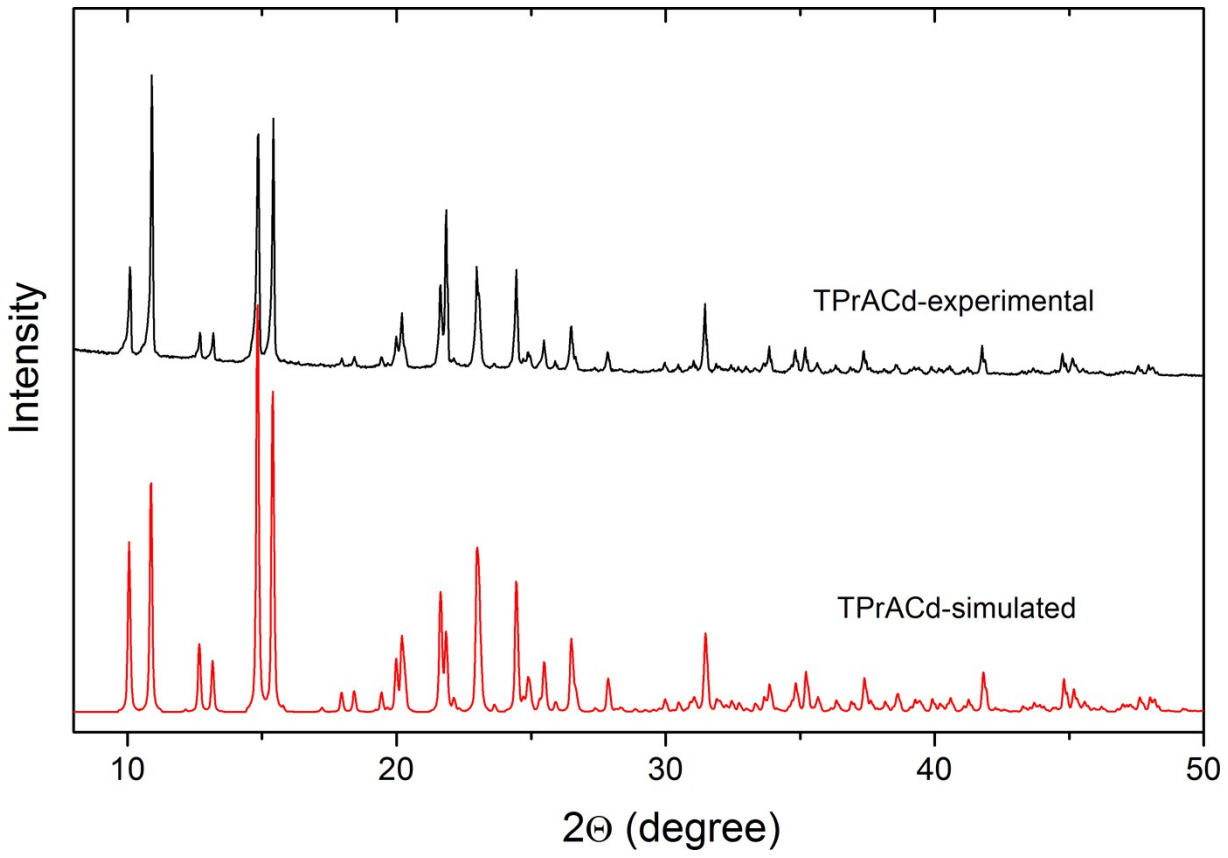

Figure S1. Room-temperature powder XRD pattern for the as-prepared sample together with the calculated one based on the single crystal structure.

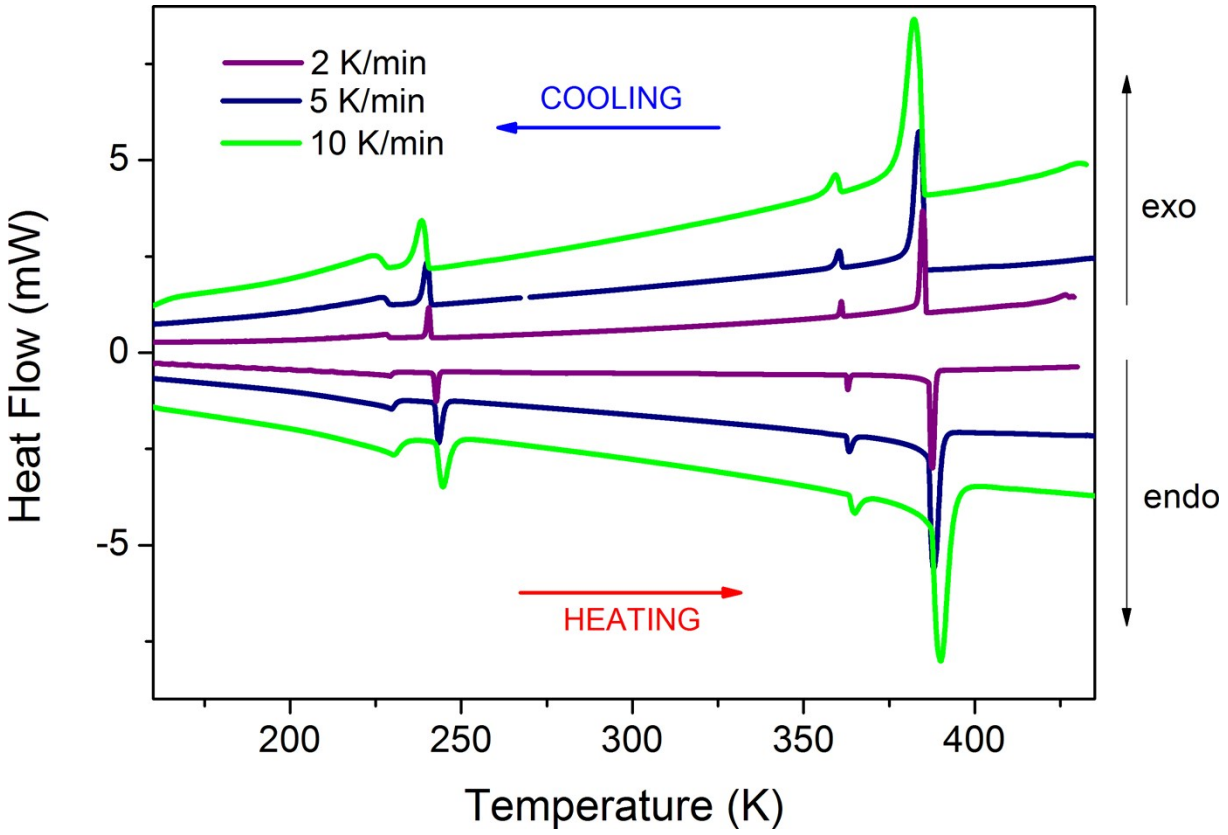

Figure S2. DSC traces for the prepared sample in heating and cooling modes at different sweeping rates.

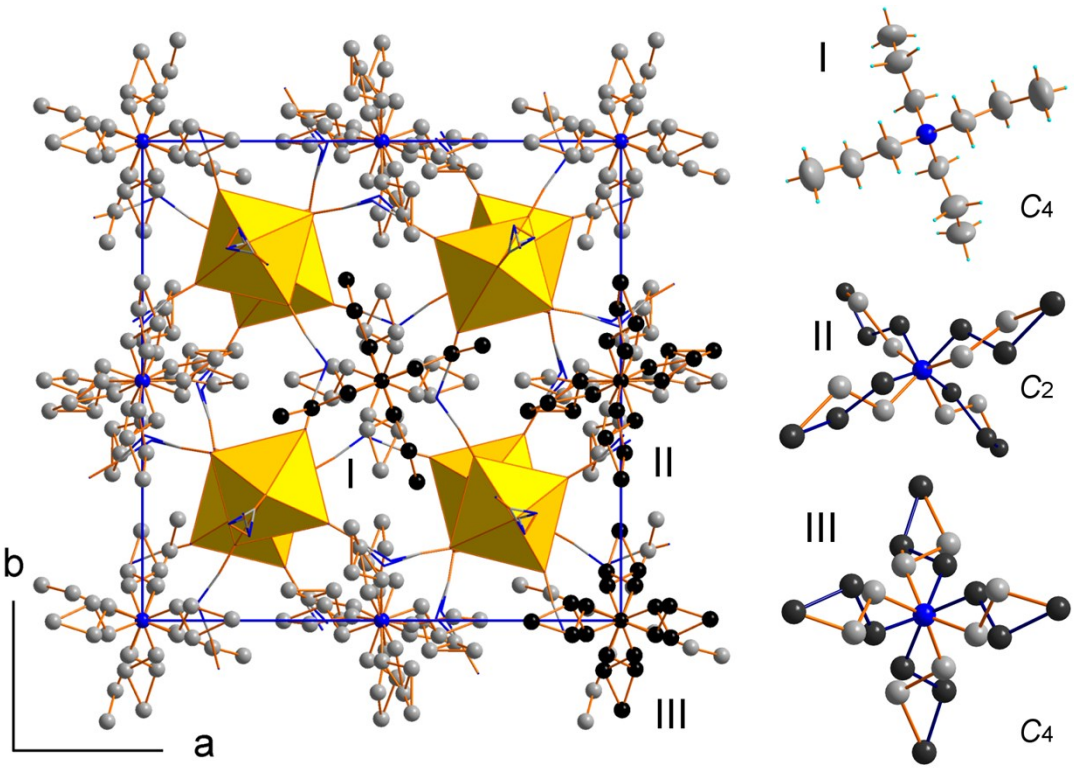

Figure S3. The crystal structure packing of the room temperature tetragonal *P*-42$_1$*c* phase of [TPrA][Cd(dca)$_3$] and three independent TPrA$^+$ cations, the alternative positions are marked on dark gray, all split carbon atoms are occupied with 0.5 probability.

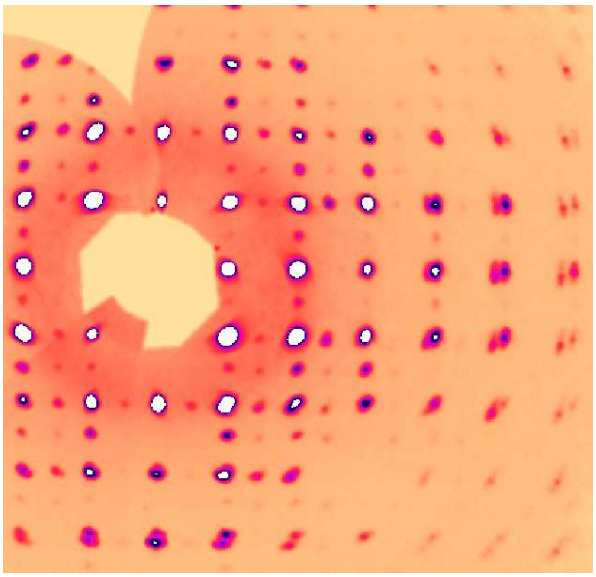

Fig S4. Reciprocal space reconstruction in phase P0a at 233 K.

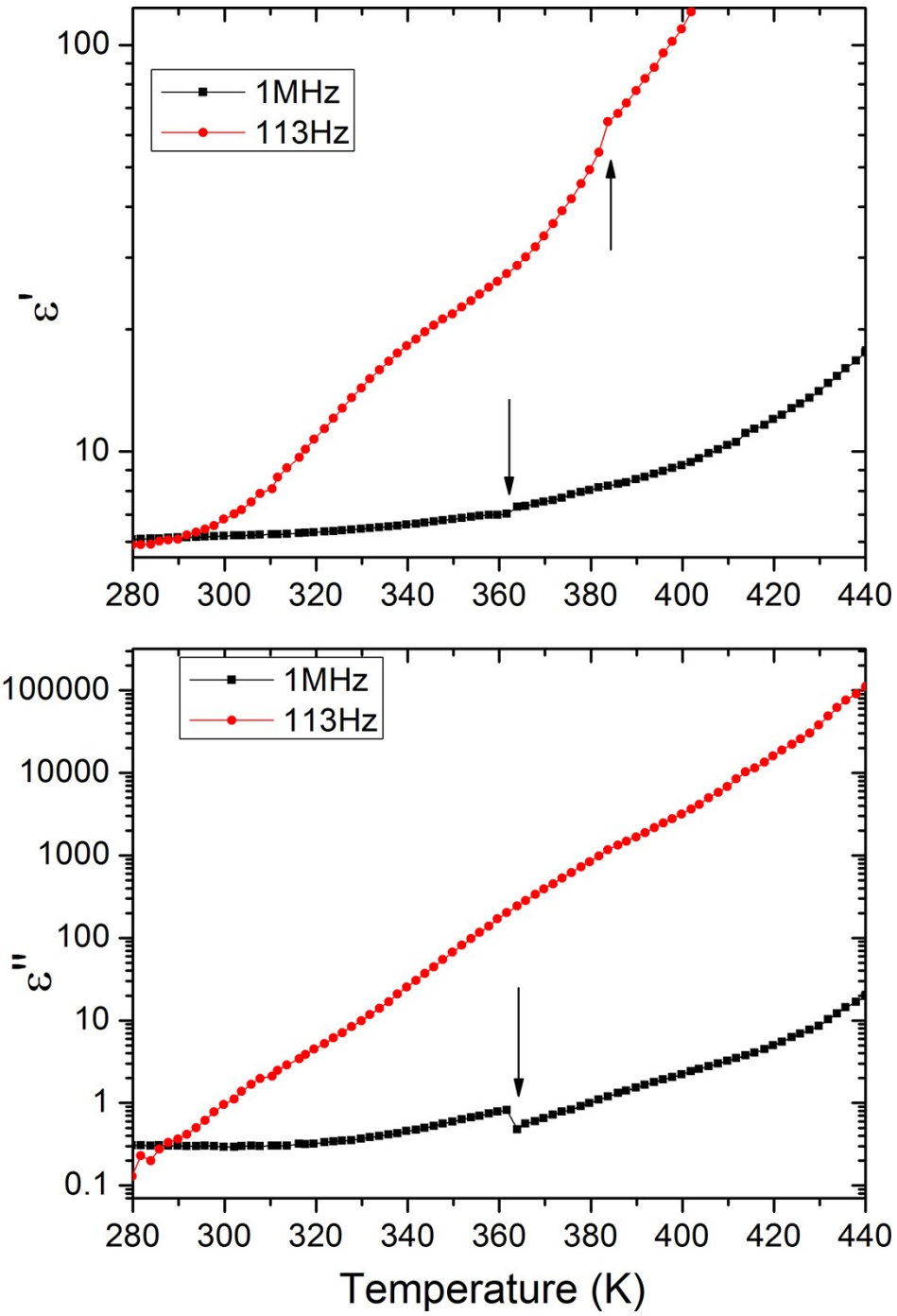

Figure S5. Temperature dependence of real and imaginary parts of the dielectric permittivity of [TPrA][Cd(dca)$_3$] single crystal at 1 MHz and 113 Hz showing small anomalies at 363 and 385 K.

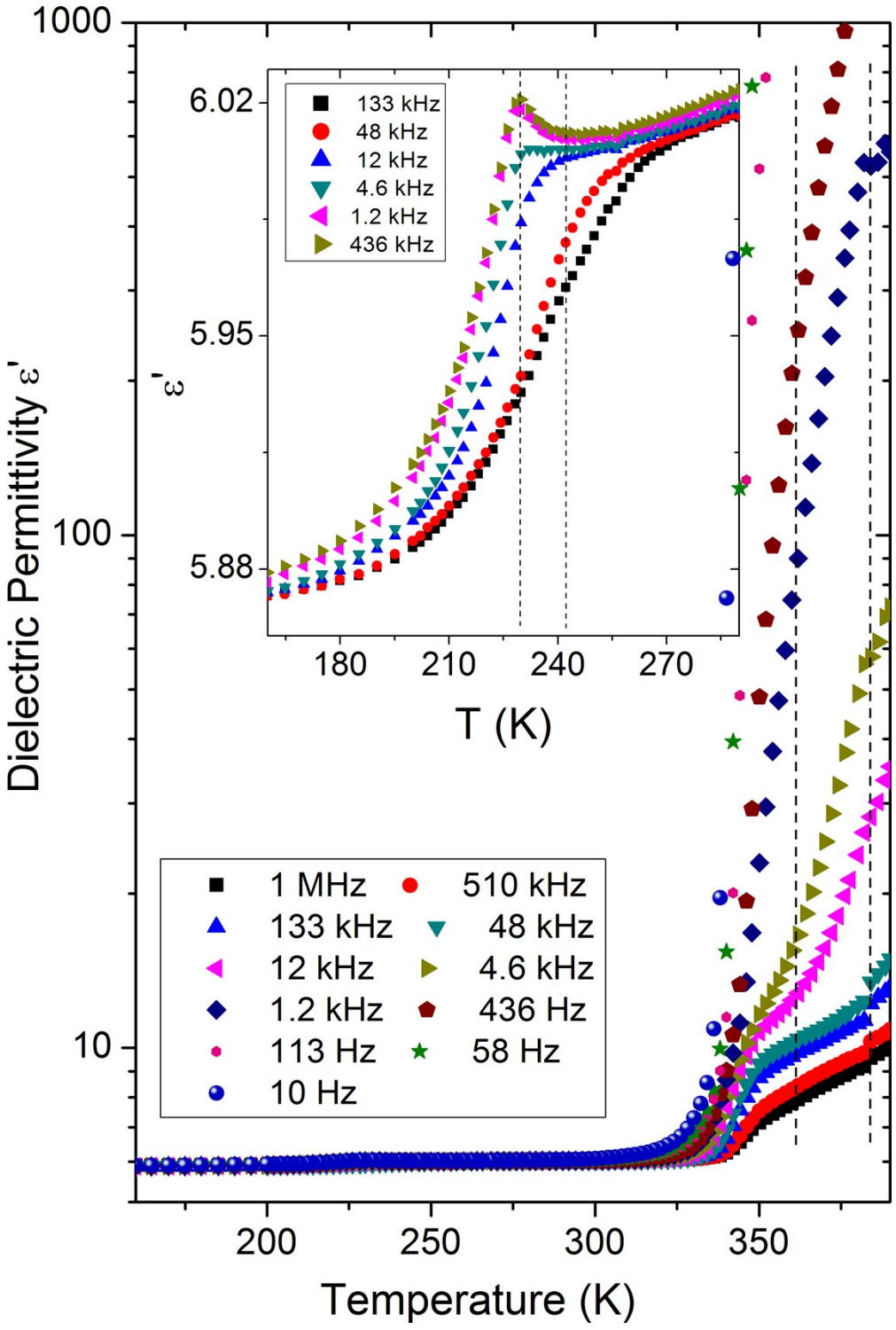

Figure S6. Temperature dependence of real part of the dielectric permittivity of [TPrA][Cd(dca)$_3$] (pelettized sample). Vertical lines correspond to temperatures at which phase transitions occur.

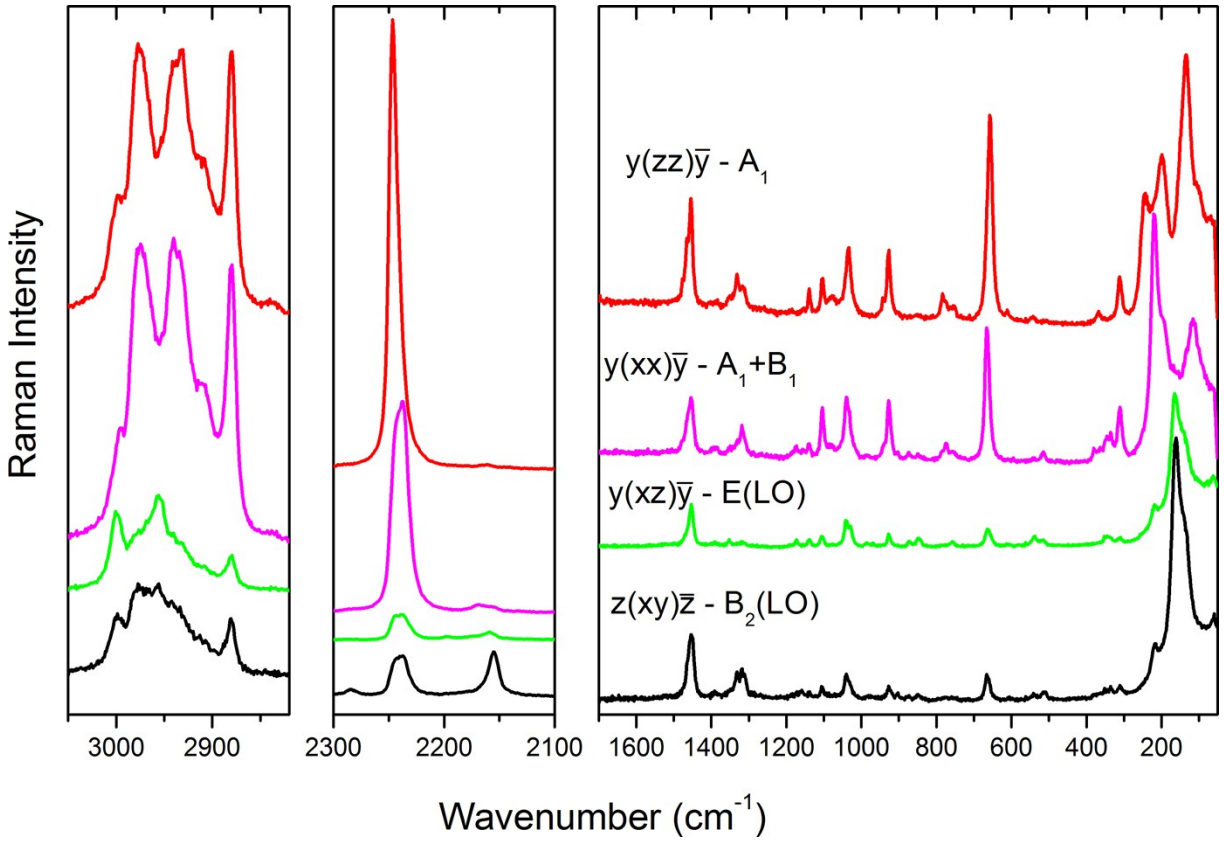

Figure S7. Polarized Raman spectra of [TPrA][Cd(dca)$_3$].

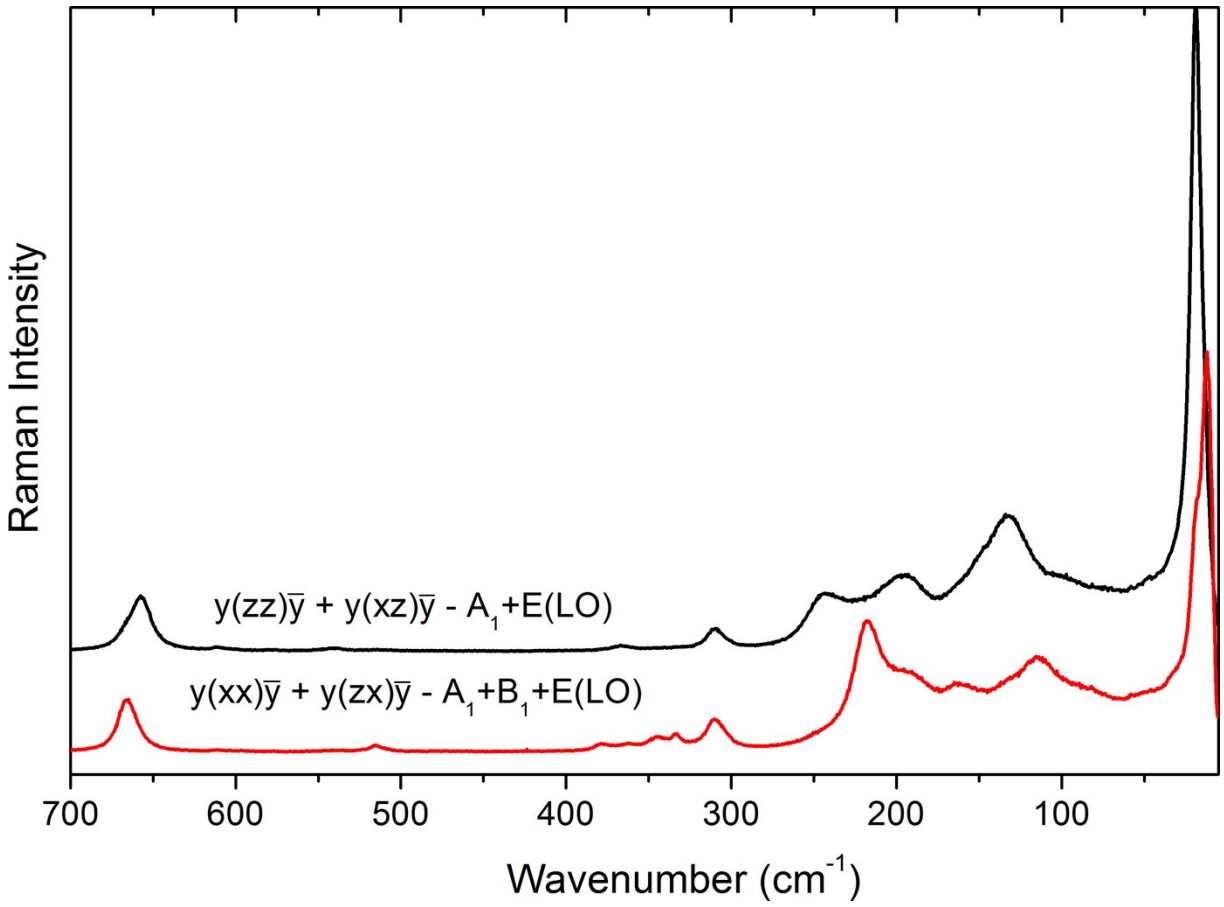

Figure S8. Raman spectra of [TPrA][$Cd(dca)_3$] measured with use of eclipse filter to show low-wavenumber region down to 5 cm^{-1}.

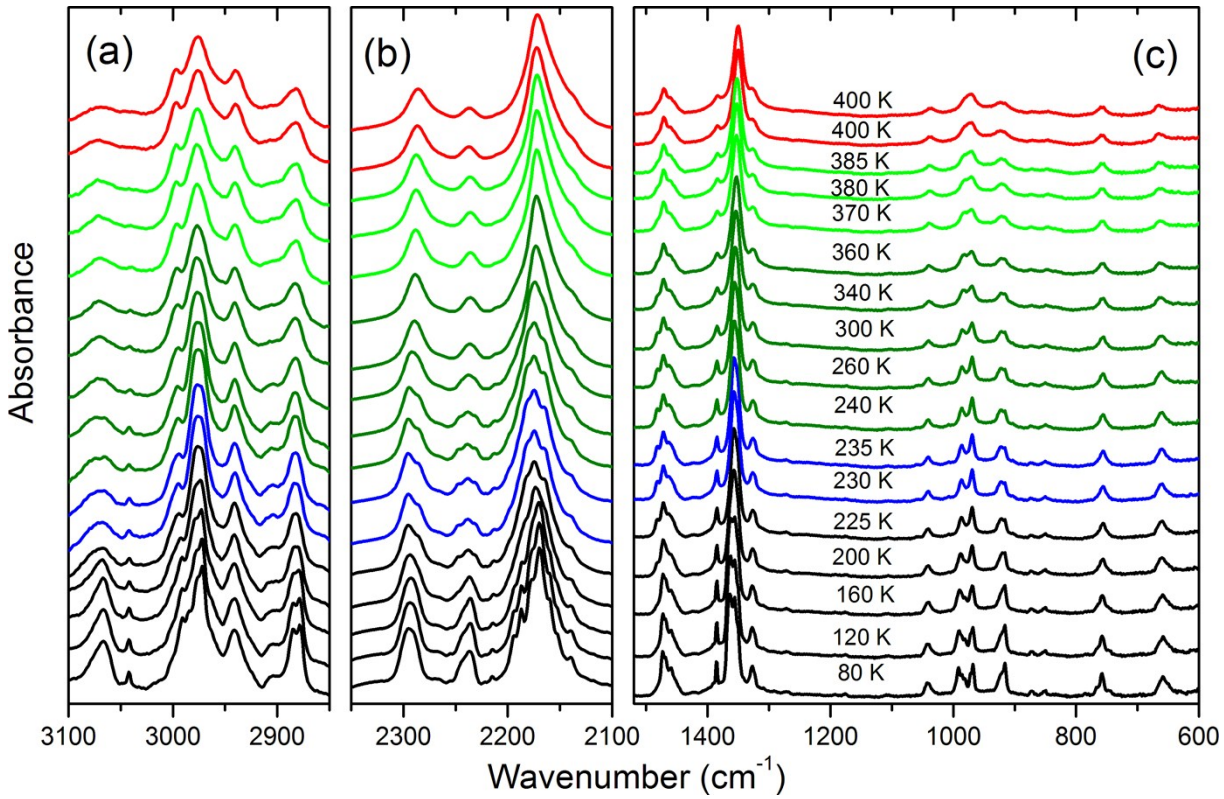

Figure S9. Temperature-dependent IR spectra of [TPrA][Cd(dca)$_3$].

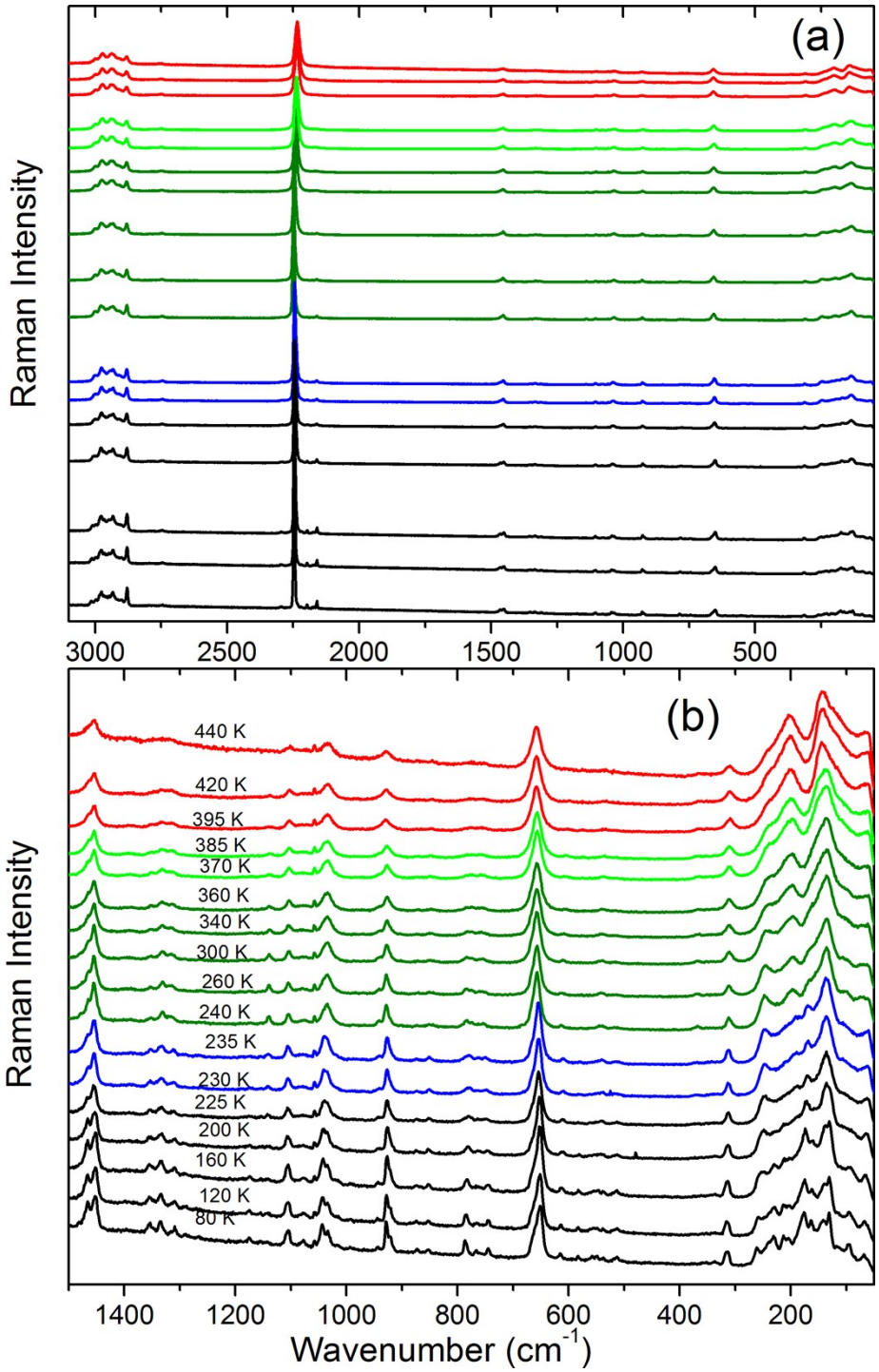

Figure S10. Temperature-dependent Raman spectra of $[TPrA][Cd(dca)_3]$ in the whole wavenumber range corresponding to polarization y(zz)y+y(xz)y.

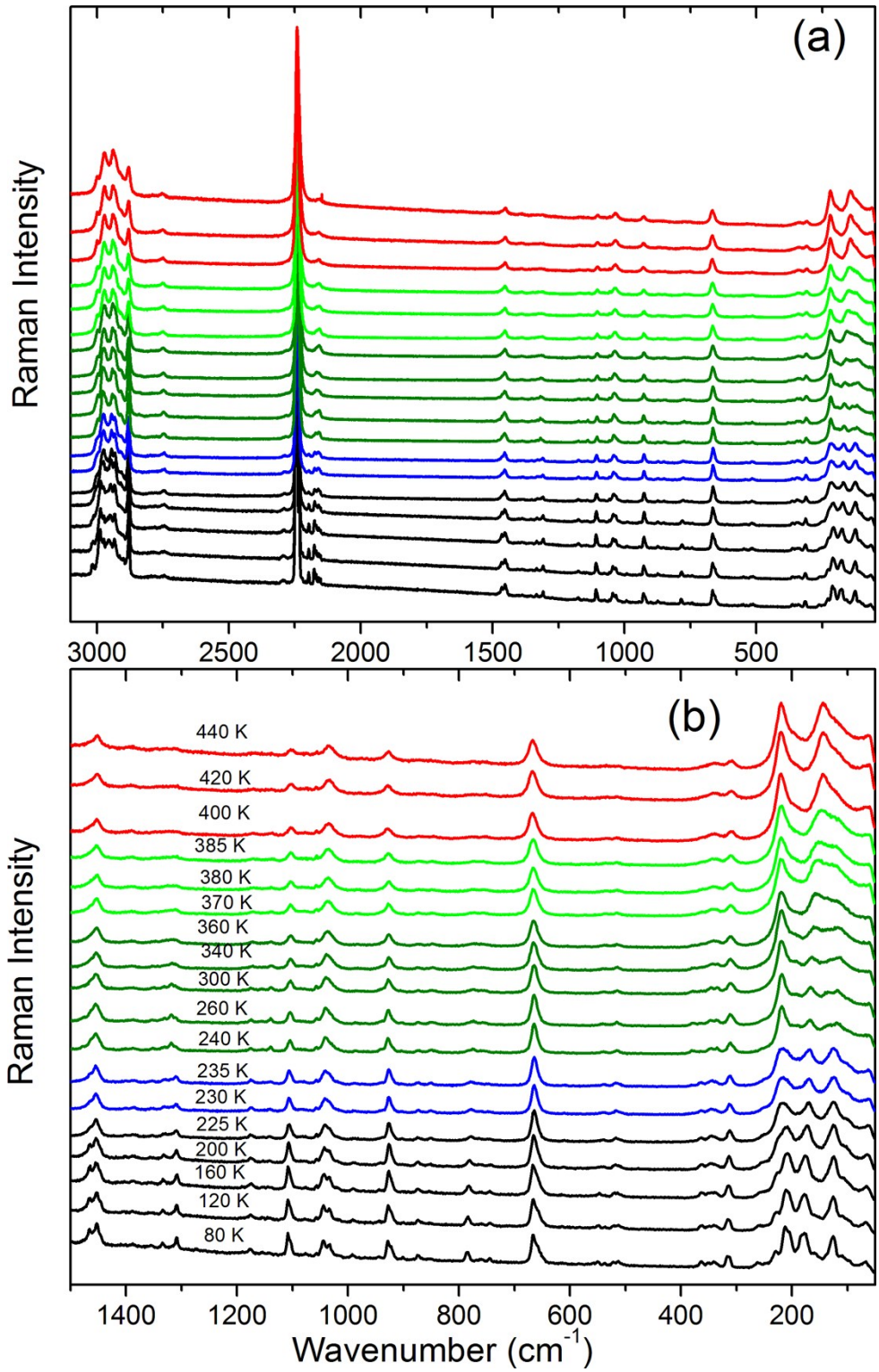

Figure S11. Temperature-dependent Raman spectra of [TPrA][Cd(dca)$_3$] in the whole wavenumber range corresponding to polarization y(xx)y+y(zx)y.

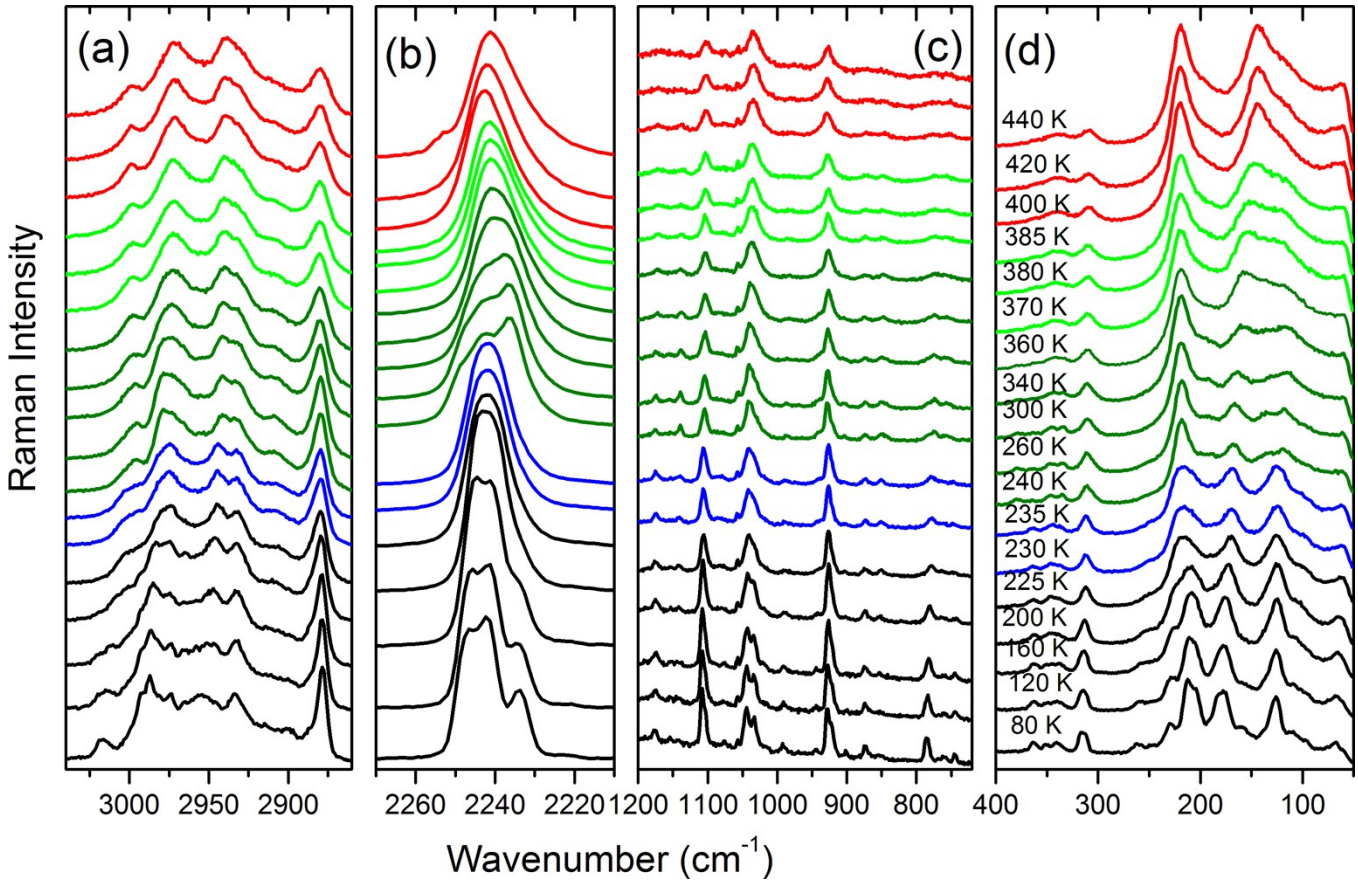

Figure S12. Details of the temperature-dependent Raman spectra of $[TPrA][Cd(dca)_3]$ corresponding to polarization y(xx)y+y(zx)y and the spectral ranges 3040-2860, 2270-2210, 1200-720 and 400-50 cm^{-1}.

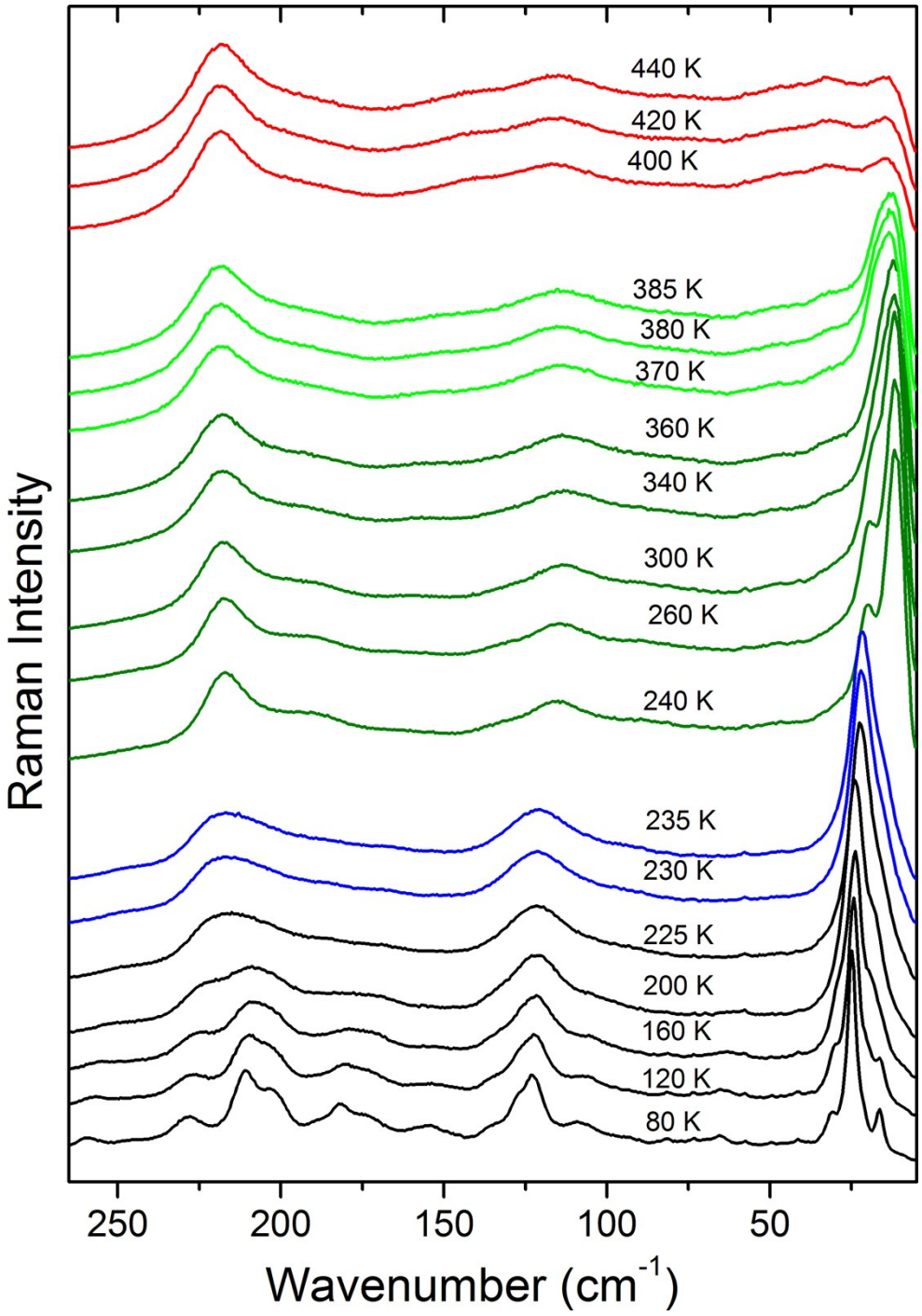

Figure S13. Temperature-dependent Raman spectra of [TPrA][Cd(dca)$_3$] measured with use of the eclipse filter in polarization y(xx)y+y(zx)y in the 5-265 cm^{-1} range.

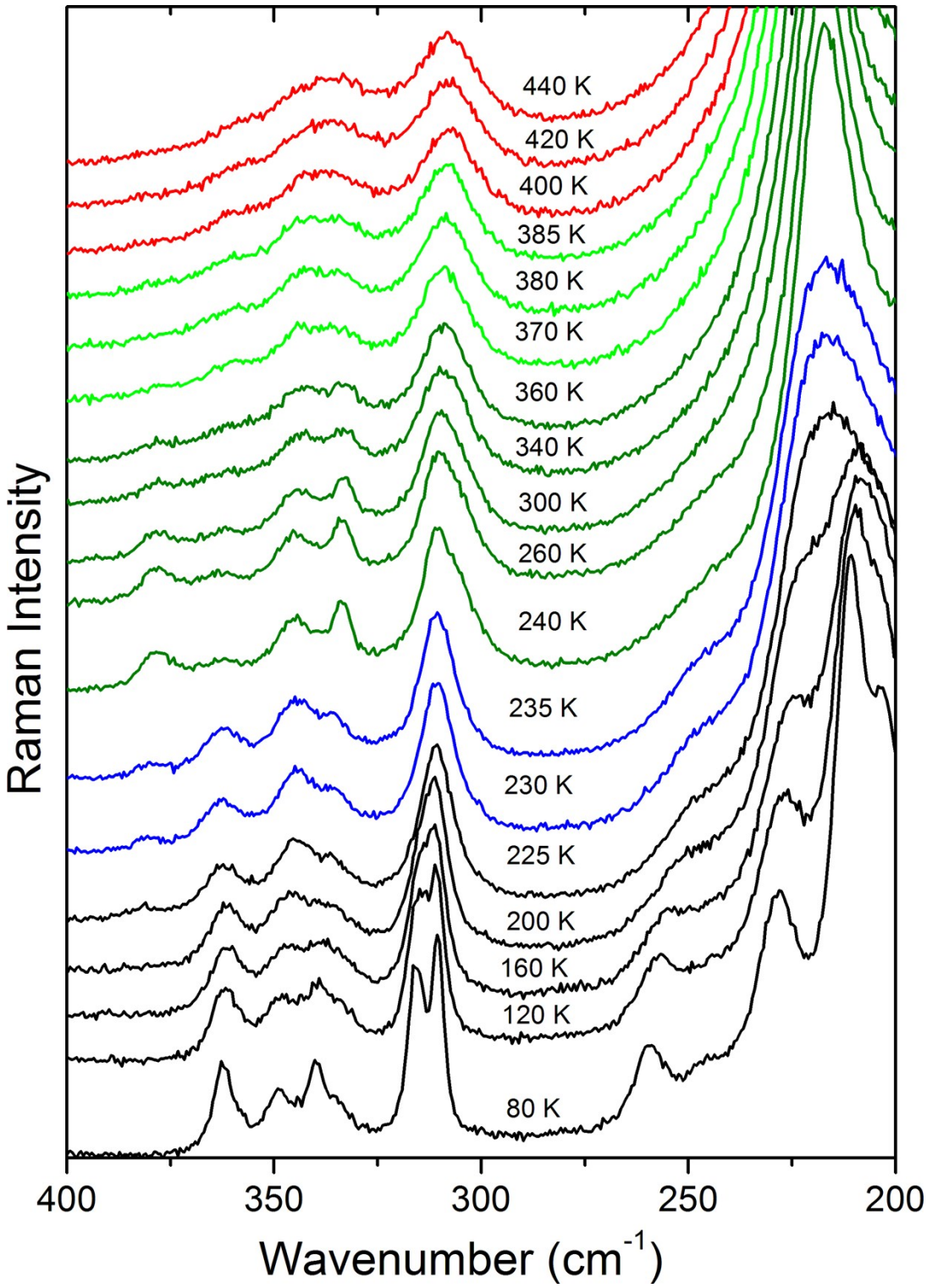

Figure S14. Temperature-dependent Raman spectra of [TPrA][Cd(dca)$_3$] measured with use of the eclipse filter in polarization y(xx)y+y(zx)y in the 200-400 cm^{-1} range.

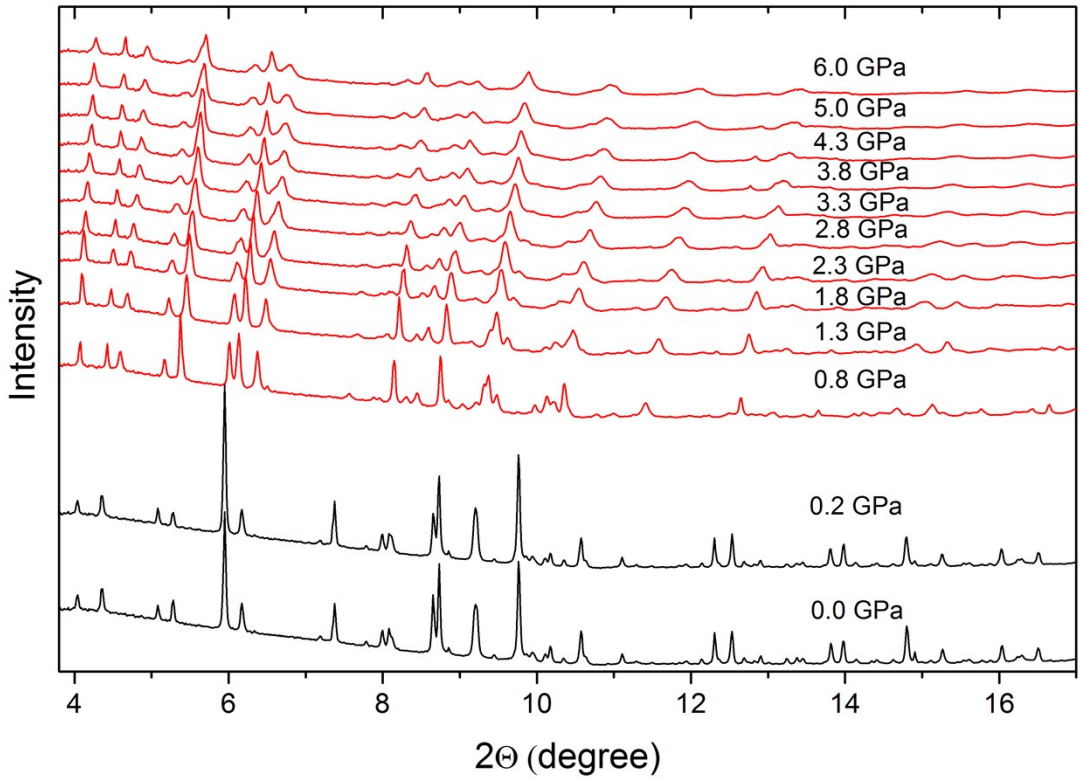

Figure S15. Pressure-dependent X-ray diffraction patterns of [TPrA][Cd(dca)$_3$] measured with use of the eclipse filter in polarization y(xx)y+y(zx)y.

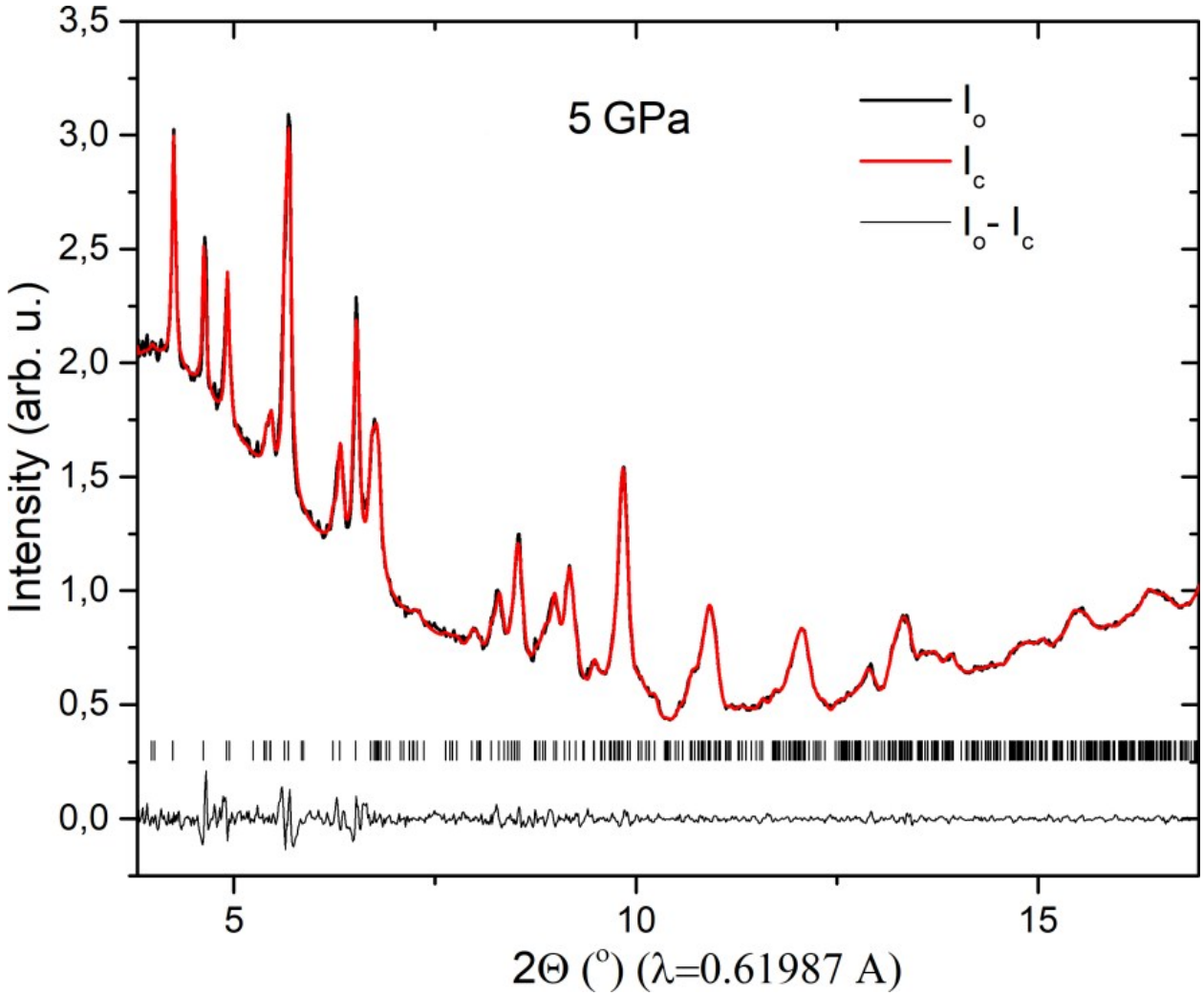

Figure S16. The Le Bail refinement with Jana 2006 (Petricek, V., Dusek, M. & Palatinus L. (2014). Z. Kristallogr. 229(5), 345-352) of profile parameters for $[TPrA][Cd(dca)_3]$ compressed at 5.0 GPa. The unit cell parameters are: 15.368(1) Å,14.362(1) Å, 16.725(1) Å, β=90.86890, V=3691.3(1)Å^3. GOF=0.02 Rp=1.17 wRp=1.72 (λ=0.61987 Å).

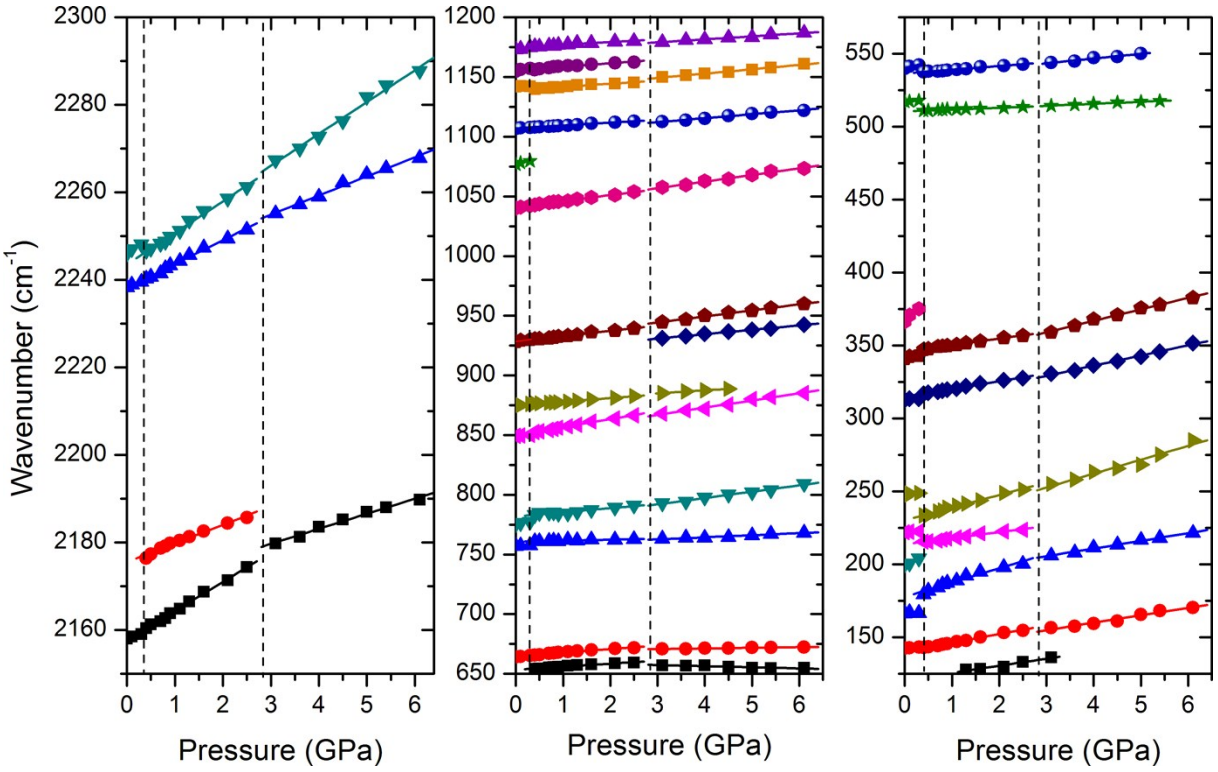

Figure S17. Wavenumber vs. pressure plots of the Raman modes observed in $[TPrA][Cd(dca)_3]$ crystal for compression experiment. The solid lines are linear fits on the data to $\omega(P) = \omega_0+\alpha P$. Vertical lines show the pressure at which structural changes occurs.

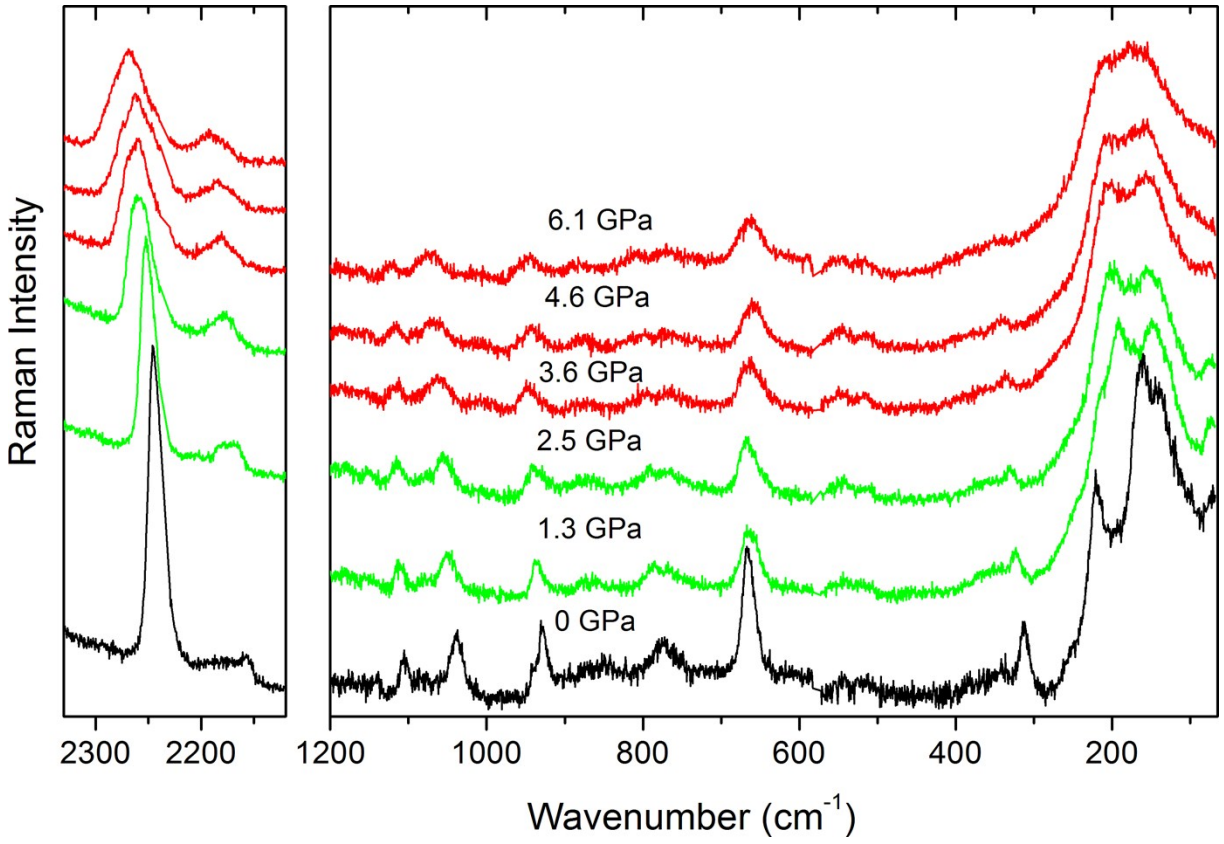

Figure S18. Raman spectra of [TPrA][Cd(dca)$_3$] duriing the decompression experiment.